Coherent population transfer of ground-state atoms into Rydberg states

T. Cubel, B. K. Teo, V. S. Malinovsky,* J. R. Guest,† A. Reinhard, B. Knuffman, P. R. Berman, and G. Raithel
FOCUS Center and Michigan Center for Theoretical Physics, Department of Physics, University of Michigan, Ann Arbor, Michigan 48109, USA
(Received 1 February 2005; published 8 August 2005)

The technique of stimulated Raman adiabatic passage (STIRAP) is used to excite laser-cooled rubidium atoms from the ^{85}Rb $5S_{1/2}$ ground state to the $44D_{5/2}$ Rydberg state through the $5P_{3/2}$ state. The utilized double-STIRAP scheme allows for an accurate determination of the absolute excitation efficiency. Experimental data are compared with results of a detailed theoretical model, and good agreement is found. It is concluded that at the center of the excitation region an excitation efficiency of 70% is achieved.

DOI: 10.1103/PhysRevA.72.023405 PACS number(s): 32.80.Rm, 32.80.Pj, 42.50.Hz

Rydberg atoms have potential applications as elements in fast quantum gates [1] and in reliable single photon sources [2], as well as in the generation of mesoscopic entanglement [3]. Critical to these applications is the large electric-dipole interaction between Rydberg atoms. In experimental realizations of these and other proposals, it will be essential to have methods available to efficiently transfer ground-state atoms into and out of Rydberg levels. Rydberg-atom excitation with π-pulses has been demonstrated [4], but was achieved using a laser with a large spectral width. Using such a laser, it would not be possible to achieve sufficient spectral resolution to exploit electric-dipole interactions between Rydberg atoms ($\sim$50 MHz for $n\sim40$ Rydberg atoms separated by 5 μm). Instead, π-pulses derived from a narrow-linewidth laser could, in principle, be used. However, the transfer efficiency achieved with π-pulses suffers from a high sensitivity to spatial laser-pulse inhomogeneities and other instabilities, such as variations of laser power and frequency [5]. Stimulated Raman adiabatic passage (STIRAP) is an alternative technique that is more robust and can also be implemented on short time scales. A more detailed discussion on the benefits of using STIRAP as opposed to π pulses is provided by Shore *et al.* [6].

STIRAP is a modern technique employed widely to coherently transfer population in a three-level Λ system [7]. It is achieved using a counterintuitive pulse sequence in which the Stokes pulse precedes the pump pulse and both pulses are tuned to resonance. STIRAP is equally appropriate for a ladder system, such as in the experiment discussed here. In our experiment, population is adiabatically transferred from the ^{85}Rb ground state $5S_{1/2}|F=3,m_F=3\rangle$ to the $44D_{5/2}|F''=5,m_F''=5\rangle$ Rydberg state, with negligible population in the rapidly decaying intermediate state $5P_{3/2}|F'=4,m_F'=4\rangle$ [see Fig. 1(a)]. Ideally, in the adiabatic limit almost 100% of the population can be transferred to the target state. Dynamics and target state populations are insensitive to moderate changes in pulse parameters such as pulse length, amplitude, and rise times. Population transfer to the ^{85}Rb 5D state using STIRAP has been demonstrated by Suepitz *et al.* [8]. STIRAP excitation to high-lying Rydberg states is, in principle, also possible. However, this task is challenging because of the low oscillator strength of optical Rydberg transitions.

In this paper we use STIRAP to excite the $44D_{5/2}$ Rydberg state of ^{85}Rb using a low-pressure vapor-cell magneto-optical trap (MOT). At the beginning of each experimental cycle the MOT is loaded for 10 ms. The MOT field gradient is 50 G/cm, which is higher than usual and results in a small atom cloud with a full diameter of $\sim$200 μm and an estimated density of 10^9 cm^{-3}. Under these conditions, we have not detected any radiation trapping that would influence the wave function evolution in the STIRAP process. (For larger MOTs, we observed clear evidence of radiation trapping.) The red STIRAP laser light, resonant with the $5S\rightarrow5P$(lower) transition, is obtained from an external cavity diode laser with a linewidth of $\approx$2 MHz. The intensity of this red laser pulse is homogeneous over the entire MOT atomic cloud. The blue STIRAP laser light, resonant with the $5P\rightarrow44D$(upper) transition, is obtained from a frequency doubled 960 nm laser (Toptica, TA-SHG100). It is locked to a pressure-tuned Fabry-Perot interferometer [9] and has a linewidth of $\approx$5 MHz [10]. The blue laser beam counterpropagates with the red one, is focused to a spot 30 μm in diameter at the center of the atomic cloud, and has a Ray-

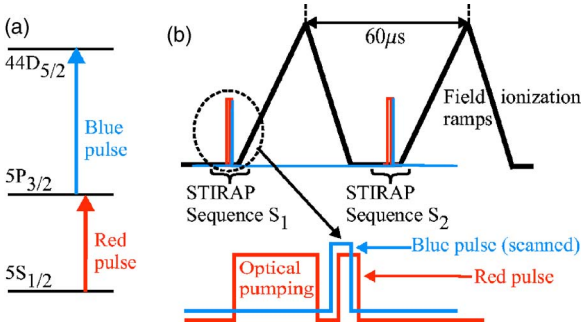

FIG. 1. (Color online) (a) Level diagram; (b) experimental timing diagram showing two STIRAP and field-ionization sequences. Two identical sequences, S_1 and S_2, are required to provide a reliable measure of the excitation efficiency.

*Present address: MagiQ Technologies, Inc., 171 Madison Avenue, Suite 1300, New York, NY 10016.

†Present address: Physics Division, Argonne National Laboratory, Argonne, IL 60439.

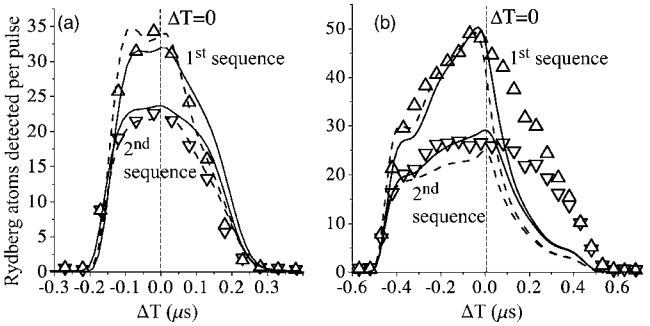

FIG. 2. Number of Rydberg atoms detected after the first (triangles up) and the second (triangles down) STIRAP sequence *vs* time delay ΔT between laser pulses for pulse durations of 0.2 μs (a) and 0.5 μs (b). The experimental results are compared with theory for a lower-transition Rabi frequency of 10 MHz and upper-transition Rabi frequencies of $\Omega_b^0/(2\pi)=7.5$ MHz (dashed lines) and 5 MHz (solid lines).

leigh length of $\sim$1.5 mm. The focusing is necessary to achieve sufficiently high Rabi frequencies on the upper transition. For the described STIRAP beam alignment and small MOT size, the Rabi frequency of the lower transition has no spatial dependence, while the Rabi frequency of the upper transition depends only on the distance r from the axis of the blue laser beam.

The STIRAP laser beams are σ^+-polarized in order to couple the states $5S_{1/2}|F=3,m_F=3\rangle$, $5P_{3/2}|F'=4,m_F'=4\rangle$, and $44D_{5/2}|F''=5,m_F''=5\rangle$. An additional σ^+-polarized $5S \rightarrow 5P$ light pulse is used to optically pump the ground state population into the $5S_{1/2}|F=3,m_F=3\rangle$ state prior to the STIRAP excitation [see Fig. 1(b)]. Under these conditions, the atoms can be modeled as three level systems, thereby greatly simplifying the theoretical analysis. All laser pulses are generated using acousto-optical modulators (AOMs). The laser pulses have negligible timing uncertainty and rise and fall times of 50 ns, limited by the AOM performance.

The experiment runs at a 20 Hz repetition rate. The MOT light is turned off 260 μs before and is turned back on 20 μs after the STIRAP excitation and Rydberg-atom detection sequences [see Fig. 1(b)]. The MOT magnetic field is left on at all times. In order to establish the excitation efficiency, the experiment employs two consecutive sequences of STIRAP excitation and Rydberg-atom detection, applied to the same atom sample (i.e., without intermediate turn-on of the MOT lasers). After each STIRAP sequence, a field ionization pulse is applied to internal electrodes, to ionize all Rydberg atoms excited in the preceding STIRAP sequence. The liberated electrons are detected on a microchannel plate (MCP) detector. During the field ionization, all Rydberg atoms are removed from the atomic cloud. Since the second STIRAP pulse sequence starts with the ground-state population left over after the first sequence, the Rydberg signal detected after the second sequence is reduced relative to that after the first sequence. This signal reduction is a robust measure for the absolute efficiency of the Rydberg atom excitation.

Figure 2 shows the number of Rydberg atoms detected after the two STIRAP excitation sequences versus the delay ΔT of the blue STIRAP pulse relative to the red one. A negative value of ΔT corresponds to a "counterintuitive" pulse sequence, in which the blue pulse precedes the red one. The blue-pulse delay is scanned in steps of 0.05 μs. Red and blue pulses have identical durations [0.2 μs in Fig. 2(a) and 0.5 μs in Fig. 2(b)]. As expected for STIRAP, the population transfer is most efficient when the blue laser pulse precedes the red laser pulse; highest yields are obtained for pulse delays $-0.1\ \mu\text{s} \lesssim \Delta T \lesssim 0$ in Fig. 2(a). This behavior is seen in the Rydberg-atom counts after both the first and the second STIRAP sequence.

The number of Rydberg atoms after the second STIRAP sequence is greatly depleted with respect to the number after the first one (see Fig. 2). This behavior is observed for both 0.2 and 0.5 μs laser pulse durations, and, generally, it is more prominent for larger numbers of Rydberg atoms. An excitation efficiency $\bar{\eta}$ equivalent to the Rydberg-atom excitation probability averaged over the volume of significant excitation can be derived as follows. Assuming a spatially homogeneous excitation, the number of Rydberg atoms after the first STIRAP sequence is $S_1=\bar{\eta}N_0$, where N_0 is the initial number of ground-state atoms in the excitation volume. The number of Rydberg atoms detected after the second, identical excitation sequence is $S_2=\bar{\eta}(N_0-S_1)=\bar{\eta}N_0(1-\bar{\eta})$. Thus, $\bar{\eta}=1-S_2/S_1$. Using the STIRAP data obtained with the 0.5 μs pulses, we find $\bar{\eta}=50\%\pm5\%$ on the counterintuitive side of Fig. 2 (i.e., $\Delta T<0$). The described method allows us to determine $\bar{\eta}$ without knowledge of the MOT density nor the MCP detection efficiency. Since both these quantities carry large uncertainty factors, any method to derive $\bar{\eta}$ from absolute count values rather than from count ratios would result in unacceptable uncertainties for $\bar{\eta}$.

In a control experiment, we have verified that the number of Rydberg atoms counted after the second STIRAP sequence with the first blue laser pulse disabled was not less than the number after the first sequence with the blue laser pulse on. Thus, the reduction of the Rydberg-atom number in the second sequence seen in Fig. 2 is actually due to the presence of the first sequence and not due to unwanted effects such as atom-cloud expansion.

It is important to minimize atom migration effects between the two STIRAP sequences. Therefore, within the limitations imposed by the duration of the field ionization pulses, we set the time delay between the two STIRAP sequences as short as possible (60 μs). Our laser-cooled atoms are estimated to travel $\approx$6 μm between the STIRAP sequences, which is only a small fraction of the diameter of the excitation volume. Therefore, we believe that atom migration effects are minimal. Any residual effect of atom migration will result in atoms from outside the excitation volume partially filling in the deficiency in ground-state atom density left after the first STIRAP sequence, thereby reducing the difference in Rydberg atom numbers after the first and the second sequence. Atom migration will therefore result in a systematic underestimate of the efficiency $\bar{\eta}$. We also note that we could find no evidence of saturation in the Rydberg-atom detection. (Saturation would also lead to an underestimate of $\bar{\eta}$.)

Due to the dependence of the blue-laser intensity on the distance r from the axis of the blue beam, the value of $\bar{\eta}$ obtained in the above analysis is a function of the actual

Rydberg-atom excitation efficiency $\eta_a(r)$. Since $\eta_a(r)$ will generally peak near $r=0$ and rapidly fall off at larger r, the maximum of $\eta_a(r)$ is considerably larger than the value of 50% we found for $\bar{\eta}$. In the following, this is shown using a detailed model that takes the inhomogeneity of the blue laser intensity into account.

We solve the following density matrix equation for a three-level system including spontaneous decay from the intermediate level:

$$\dot{\rho}_{11} = -i\frac{\Omega_r}{2}(\rho_{12}-\rho_{21}) + \gamma\rho_{22},$$

$$\dot{\rho}_{22} = i\frac{\Omega_r}{2}(\rho_{12}-\rho_{21}) - i\frac{\Omega_b}{2}(\rho_{23}-\rho_{32}) - \gamma\rho_{22},$$

$$\dot{\rho}_{12} = i\delta_r\rho_{12} - i\frac{\Omega_r}{2}(\rho_{11}-\rho_{22}) - i\frac{\Omega_b}{2}\rho_{13} - \frac{\gamma}{2}\rho_{12},$$

$$\dot{\rho}_{13} = i\delta\rho_{13} - i\frac{\Omega_b}{2}\rho_{12} + i\frac{\Omega_r}{2}\rho_{23},$$

$$\dot{\rho}_{23} = i\delta_b\rho_{23} - i\frac{\Omega_b}{2}(\rho_{22}-\rho_{33}) + i\frac{\Omega r}{2}\rho_{13} - \frac{\gamma}{2}\rho_{23},$$

$$\dot{\rho}_{33} = -i\frac{\Omega_b}{2}(\rho_{32}-\rho_{23}), \tag{1}$$

where ρ_{ii} ($i=1$, 2, and 3) is the population of the ground ($S_{1/2}$), intermediate ($P_{3/2}$) and target ($44D_{5/2}$) Rydberg state of the Rb atom, ρ_{ij} ($i\neq j$)'s are the coherences, $\delta_{r,b}$ are the detunings of the red/blue laser pulses from lower/upper transitions, respectively, δ is the two-photon detuning, γ is the spontaneous decay rate of the $P_{3/2}$ state, and $\Omega_{r,b}$ are the Rabi frequencies of the lower/upper transitions.

The experimental signal, i.e., the total number of Rydberg atoms after the STIRAP sequences, is modeled by weighted volume integrals of $\eta_a(r)=\rho_{33}(r,t\to\infty)$. In the calculation of the latter, the value of Ω_r is assumed to be constant since the diameter of the red laser beam is much larger than that of the blue beam. The Gaussian spatial profile of the blue laser beam has been taken into account by including the corresponding dependence of Ω_b on the radial coordinate r. Final expressions for the Rydberg-atom yield S after STIRAP sequences 1 and 2 for the case of a Gaussian spatial profile of the blue laser beam have the forms

$$S_1 \propto \int_{\Omega_b^R}^{\Omega_b^0} \eta_a(\Omega_b)\frac{d\Omega_b}{\Omega_b}, \tag{2}$$

$$S_2 \propto \int_{\Omega_b^R}^{\Omega_b^0} \{\eta_a(\Omega_b)[1-\eta_a(\Omega_b)]\}\frac{d\Omega_b}{\Omega_b}, \tag{3}$$

where Ω_b^0 and Ω_b^R are the Rabi frequencies of the upper transition at $r=0$ and at a cutoff distance $r=R$, respectively. Results do not significantly depend on the choice for Ω_b^R.

The calculations based on Eqs. (1)–(3) require input values for the constant Rabi frequency of the lower transition, Ω_r, and the central Rabi frequency of the upper transition, Ω_b^0. Using measurements of the Autler-Townes splitting on the lower transition [10], the value of $\Omega_r/(2\pi)$ was experimentally determined to be 10 MHz±1 MHz. Due to the spatial inhomogeneity of the blue laser beam, it has been more difficult to estimate Ω_b^0. We have estimated Ω_b^0 by measurements of light-induced Rydberg-atom quenching, observed when the blue light is left on after the red light has been turned off. In Fig. 3(a), the red and blue laser pulses are turned on during time intervals extending from 0.2 to 0.4 μs and from 0 to t, respectively. The turn-off time of the blue pulse is varied from 0.2 to 1.5 μs. Once the blue laser pulse extends past the red laser pulse, Rydberg atoms are coupled back into the $5P$ state where they quickly decay back into the $5S$ ground state. The quenching rate is determined by the spatially inhomogeneous Ω_b. Due to the Gaussian profile of the blue beam, Rydberg atoms near the beam axis are quenched rapidly, causing a rapid initial drop of the Rydberg signal in the interval 0.4 μs$<t\lesssim$0.5 μs of Fig. 3(a). Rydberg atoms in the wings of the blue beam are quenched more slowly, causing a continued but slow decrease of the Rydberg population at $t\gtrsim 0.5$ μs. Quantitatively, we have modeled the quenching by solving approximate differential equations for the amplitudes of the Rydberg and the $5P$ levels, $\dot{b}_3 = i(\Omega_b/2)e^{-z^2}b_2$ and $\dot{b}_2 = i(\Omega_b/2)e^{-z^2}b_3 - \gamma b_2/2$, respectively, and weighted spatial integration. Results for $\Omega_b^0/(2\pi)=5$, 7.5, and 10 MHz are shown in Fig. 3(a). Based on such calculations, we estimate 5 MHz$\lesssim\Omega_b^0/(2\pi)\lesssim$10 MHz for our experiment. This is in reasonable agreement with beam diameter, laser power, and dipole moment (calculated value 0.03 atomic units).

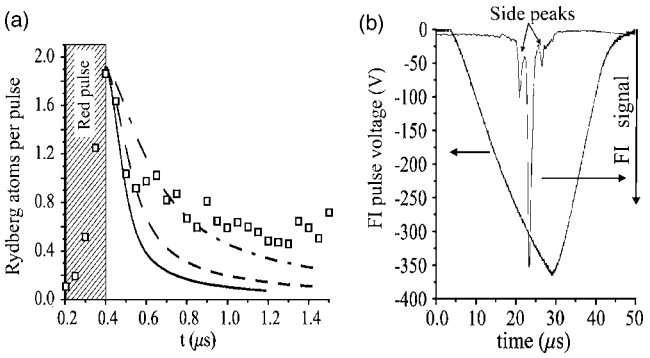

FIG. 3. (a) Laser-induced Rydberg-atom quenching. The lower-transition red laser pulse is on from $t=0.2$ to 0.4 μs, and the upper-transition blue laser pulse from 0 to t (x-coordinate of the plot). Rydberg-atom quenching occurs for $t>0.4$ μs. Measurements (squares) and simulations for $\Omega_b^0/(2\pi)=5$, 7.5, and 10 MHz (dot-dashed, dashed, and solid curves, respectively) are shown; (b) field ionization pulse and field-ionization spectrum for $\Delta T=0$ and laser pulse width of 0.5 μs. The $44D$ state ionizes at ~310 V.

Using Ω_b^0 values in that range and $\Omega_r/(2\pi)=10$ MHz, as well as experimentally recorded temporal pulse shapes, we have calculated S_1 and S_2 using Eqs. (1)–(3). In Fig. 2, the results for $\Omega_b^0/(2\pi)=5$ and 7.5 MHz are compared with experimental data. All theoretical STIRAP curves are displayed on identical scales. In accordance with the expected robustness of STIRAP excitation, the differences between the the-

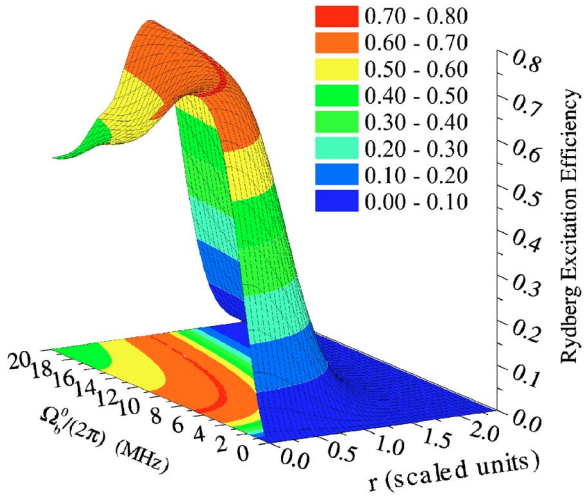

FIG. 4. (Color online) Efficiency of the Rydberg-state excitation, η_a, vs the central Rabi frequency of the upper transition, $\Omega_b^0/(2\pi)$, and distance r from the center of the blue beam. The Rabi frequency of the lower transition is 10 MHz.

oretical curves for $\Omega_b^0/(2\pi)=5$ and 7.5 MHz are quite minor. The comparison between experiment and theory shows that we are able to model our STIRAP experiment quite well. Considering the ratios between STIRAP sequences 1 and 2 and the general shape of the data, the theoretical curves for $\Omega_b^0/(2\pi)=7.5$ MHz fit the experimental data best.

Figure 4 shows the Rydberg-atom excitation efficiency η_a as a function of Ω_b^0 and r, obtained using $\Omega_r/(2\pi)=10$ MHz, experimentally recorded temporal shapes of the 0.5 μs pulses, and counterintuitive pulse ordering. We find that an excitation efficiency $\eta_a \approx 70\%$ is achieved over quite a wide range of values of $\Omega_b/(2\pi)$ centered around 7 MHz. Combining all experimental and theoretical evidence, we conclude that in our experiment the Rydberg-atom excitation efficiency achieved with STIRAP reaches a maximum of about 70% near the axis of the blue laser beam.

STIRAP is most effective in the adiabatic regime when the condition $\Omega_{\text{eff}}\Delta\tau > 10$ is satisfied, where $\Delta\tau$ is the period of overlap between the two pulses, and Ω_{eff} is an effective Rabi frequency, $\Omega_{\text{eff}}=\sqrt{\Omega_b^2+\Omega_r^2}$ [7]. Using our parameters, we find $\Omega_{\text{eff}}\Delta\tau \approx 5$ and 12 for the 0.2 and 0.5 μs pulses, respectively. We are not deeply in the adiabatic regime, but deep enough to achieve reasonably efficient STIRAP excitation. Residual nonadiabatic behavior becomes evident in the low-visibility bumps in Fig. 2, which reflect partial Rabi flopping and are consistently reproduced in the experiment, and in the unexpected drop of the excitation efficiency seen in Fig. 4 at small r and $\Omega_b^0/(2\pi) \gtrsim 8$ MHz.

We believe that the data in Fig. 2(b) for the 0.5 μs case do not follow the theory as well due to the presence of state-changing collisions, which promote the Rydberg atoms into Rydberg states that are immune to quenching by the blue laser. State-selective field ionization (FI) spectra taken after STIRAP excitation exhibit two small side peaks, which provide evidence for collisions [see Fig. 3(b)]. While these FI spectra are not consistent with electron-Rydberg collisions [11], they could indicate near-elastic collisions between Rydberg atoms of the type $44D+44D \rightarrow 42F+46P$.

In conclusion, we have used STIRAP excitation to transfer population into a single Rydberg level with an average, phenomenological efficiency of 50%. The actual position-dependent Rydberg-atom excitation efficiency was found to reach a maximum of about 70% near the center of the excitation region, and it has been found to be robust with regard to pulse length and amplitude variations. In the future, these results could be improved by using a higher-power blue laser in order to achieve larger upper-transition Rabi frequencies, and by using laser pulses with a smoother time dependence, leading to improved adiabaticity of the STIRAP. Also, complications arising from the position dependence of the upper-transition Rabi frequency can, in principle, be avoided by using atom clouds smaller than the blue-beam diameter.

This work was supported in part by NSF Grant Nos. PHY-0114336, PHY-0098016, and PHY-0245532. J.R.G. acknowledges support from the Chemical Sciences, Geosciences and Biosciences Division of the Office of Basic Energy Sciences, Office of Science, U.S. Department of Energy.

[1] D. Jaksch, J. I. Cirac, P. Zoller, S. L. Rolston, R. Cote, and M. D. Lukin, Phys. Rev. Lett. **85**, 2208 (2000).
[2] M. Saffman and T. G. Walker, Phys. Rev. A **66**, 065403 (2002).
[3] M. D. Lukin, M. Fleischhauer, R. Cote, L. M. Duan, D. Jaksch, J. I. Cirac, and P. Zoller, Phys. Rev. Lett. **87**, 037901 (2001).
[4] T. Mossberg, A. Flusberg, R. Kachru, and S. R. Hartmann, Phys. Rev. Lett. **39**, 1523 (1977).
[5] R. J. Cook and B. W. Shore, Phys. Rev. A **20**, 539 (1979).
[6] B. W. Shore, K. Bergmann, A. Kuhn, S. Schiemann, and J. Oreg, Phys. Rev. A **45**, 5297 (1992).
[7] K. Bergmann, H. Theuer, and B. W. Shore, Rev. Mod. Phys. **70**, 1003 (1998).
[8] W. Süptitz, B. C. Duncan, and P. L. Gould, J. Opt. Soc. Am. B **14**, 1001 (1997).
[9] E. Hansis, T. Cubel, J.-H. Choi, J. R. Guest, and G. Raithel, Rev. Sci. Instrum. **76**, 033105 (2005).
[10] B. K. Teo, D. Feldbaum, T. Cubel, J. R. Guest, P. R. Berman, and G. Raithel, Phys. Rev. A **68**, 053407 (2003).
[11] A. Walz-Flannigan, J. R. Guest, J.-H. Choi, and G. Raithel, Phys. Rev. A **69**, 063405 (2004).